Supplementary information

Porous reticular Co@Fe metal organic gel: dual-function simulated peroxidase nanozyme for both colorimetric sensing and antibacterial applications

Meng Wang; Xiaoguang Zhu; Yannan Yin; Guixia Ling *, Peng Zhang *

Shenyang Pharmaceutical University, No. 103, Wenhua Road, Shenyang 110016, China.

* Corresponding Author Tel. and Fax: +86-24-2398 6256

E-mail address: zhangpengspu@163.com (Peng Zhang), pharlab@163.com (Guixia Ling)

1. Materials

Hydrogen peroxide (H_2O_2, 30%), Cobaltous chloride ($CoCl_2 \cdot 6H_2O$) was purchased from Macklin Biochemical Technology Co., Ltd. (Shanghai, China). 1, 3, 5-trimeric acid (H_3BTC) was purchased from j&k chemical. Ferric chloride ($FeCl_3 \cdot 6H_2O$), 3, 3', 5, 5'-tetramethylbenzidine (TMB) were obtained from Aladdin. Citric acid (CA), Glucose, metal salts (Na^+, K^+, Mg^{2+}, Ca^{2+}, Mn^{2+}, Zn^{2+}, Ag^+, Cu^{2+}, Ni^{2+}) and other reagents were obtained from Sinopharm Chemical Reagent Co., Ltd. (China). Deionized water was used throughout the experiment. Mueller Hinton (MH) Broth was purchased from Haibo Biotechnology Co., Ltd. Agar (powder) was purchased from KERMEL. *S. aureus* and *E. coli* were purchased from Beijing Preservation Biotechnology Co., Ltd. All chemicals and reagents were used as-received without any further purification.

2. Characterizations and measurements

Absorbance values were recorded by SYNERGY type multi-function measuring instrument (BioTek, USA). The morphology of the synthesized materials was obtained using a Merlin Compact scanning electron microscope (SEM) (ZEISS, Germany). Fourier transform-infrared (FT-IR) spectra were recorded using a Bruker IFS55 spectrometer. X-ray diffraction (XRD) was performed on a SmartLab SE (Rigaku, Japan) instrument. Zeta potential data were determined by Nano-ZS90 laser particle size analyzer (Malvern, UK). Electron spin resonance spectrum (ESR) was determined by the Bruker EMX PLUS (Germany). X-ray photoelectron spectroscopy (XPS) was determined by Thermo Scientific K-Alpha (US).

3. Animals

SD rats (200 g) were obtained from the Experimental Animal Center of Shenyang Pharmaceutical University. All animal experiments throughout the study were approved by the ethics committee of Shenyang Pharmaceutical University, China.

4. Results

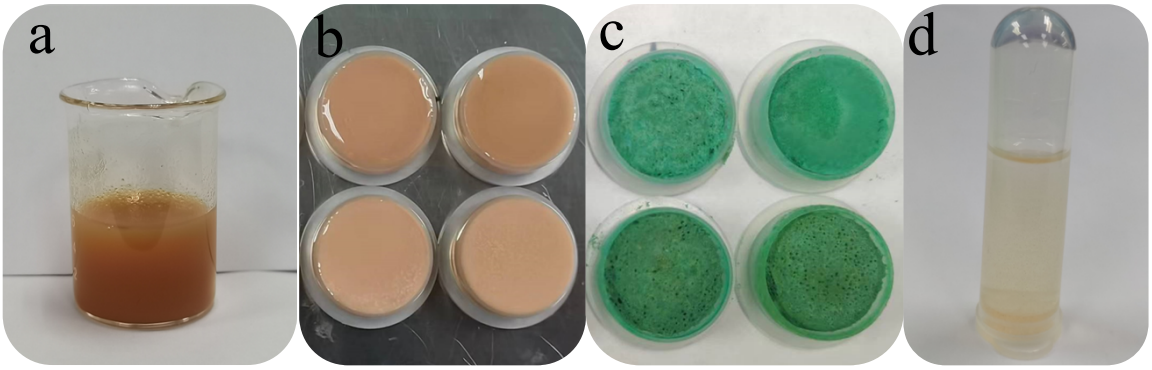

Figure S1. Physical status of Co@Fe MOG. (a) Co@Fe MOG after mixing evenly. (b) Co@Fe MOG before freeze-drying. (c) Co@Fe MOG after freeze-drying. (d) Co@Fe MOG dispersed with water.

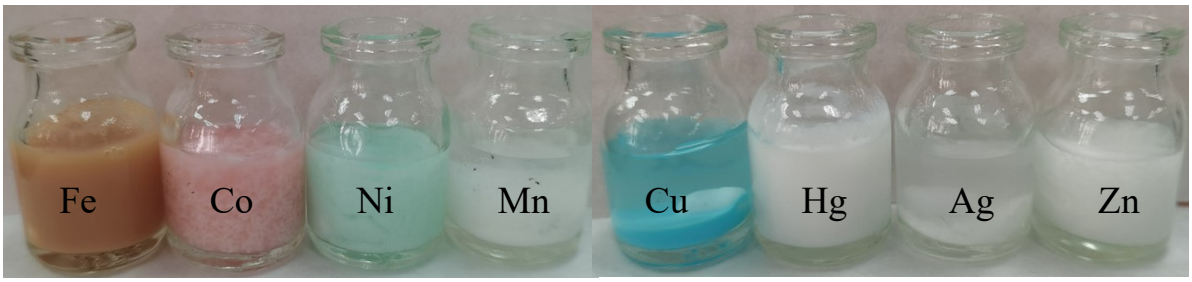

Figure S2. Physical states of MOG prepared by different metal ion sources.

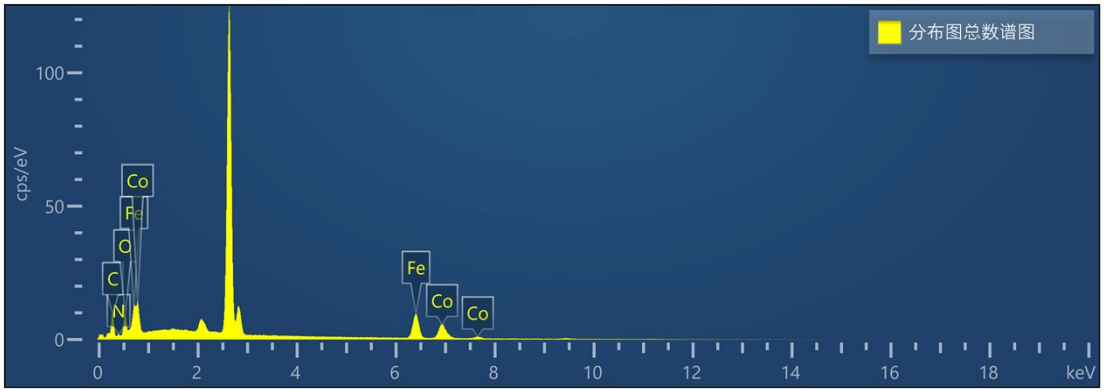

Figure S3. EDS spectrum of Co@Fe MOG showing the presence of Co, Fe, C, O, and N.

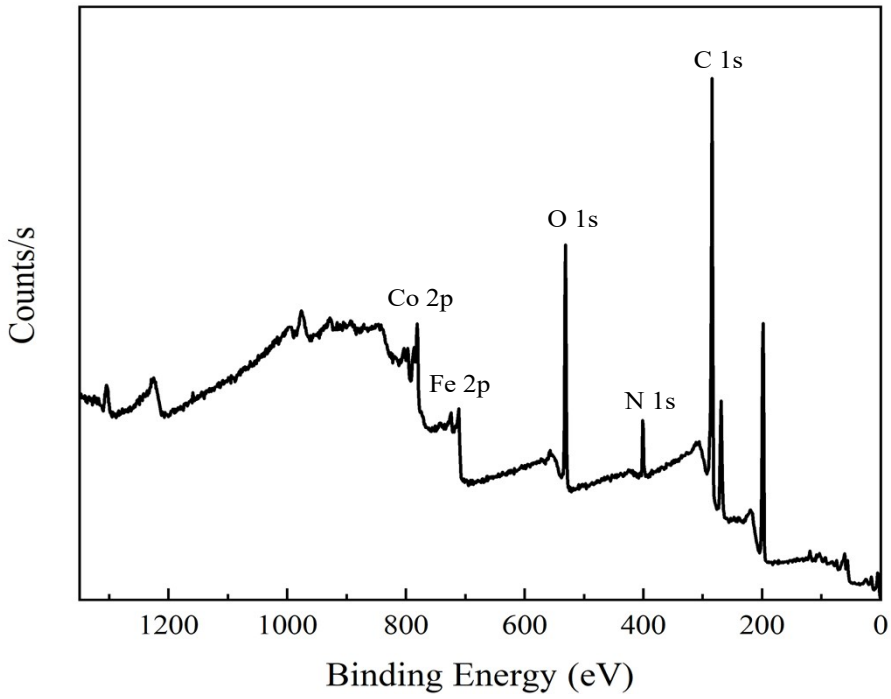

Figure S4. Spectrum of XPS full elements peak distribution.

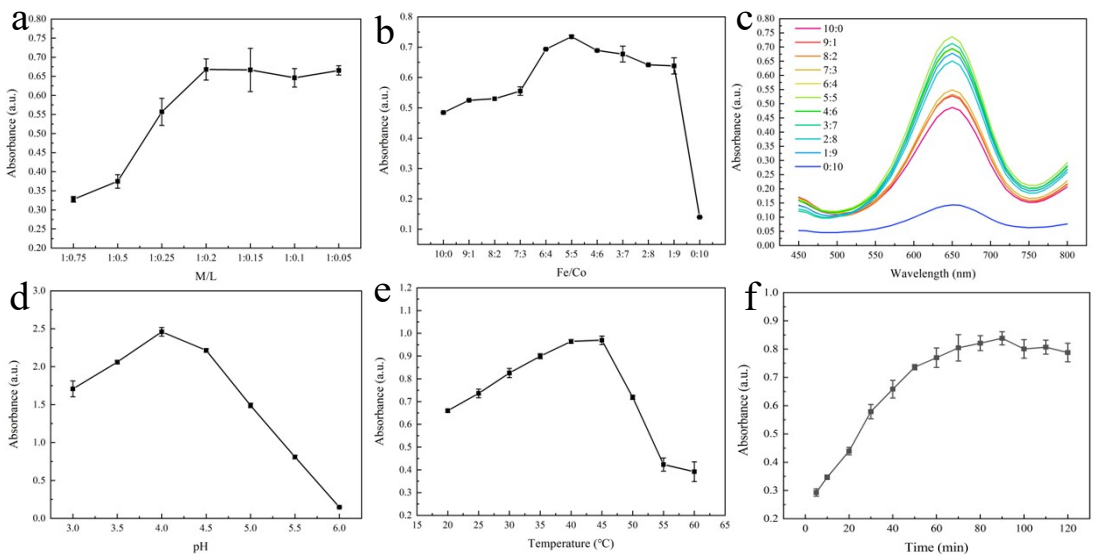

Figure S5. Optimization of experimental conditions for Co@Fe MOG-H_2O_2-TMB system. (a) Metal ligand doping ratio (M/L). (b) Metal ratio. (c) Spectral scanning of metal doping ratio. (d) pH. (e) Temperature. (f) Reaction time.

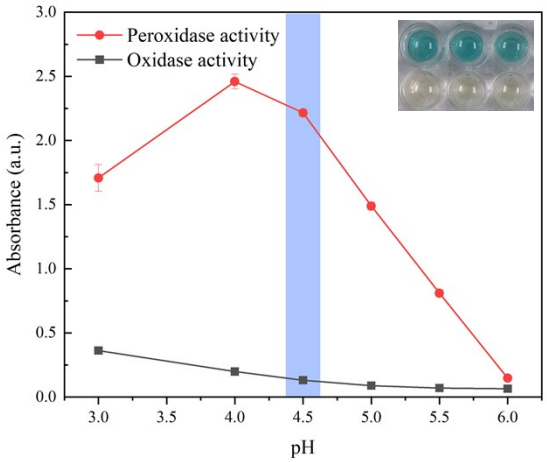

Figure S6. Comparison of peroxidase activity and oxidase activity of Co@Fe MOG at different pH.

Table S1. Comparison of physical status of MOG from different metal ion sources.

Metal	Color	Status	Mobility	A_{652} (a.u.)
$FeCl_3 \cdot 6H_2O$	Yellow	suspension	Good	1.125
$CoCl_2 \cdot 6H_2O$	Pink	Flocculation precipitation	Poor	0.333
$NiCl_2 \cdot 6H_2O$	Green	Flocculation precipitation	Poor	0.043

$C_4H_6MnO_4·4H_2O$	White	suspension	Good	0.045
$CuSO_4·5H_2O$	Blue	Flocculation precipitation	Poor	0.047
$HgN_2O_6·H_2O$	White	suspension	Poor	0.040
$AgNO_3$	White	suspension	Good	0.040
$ZnSO_4·7H_2O$	White	Flocculation precipitation	Poor	0.038

Table S2. EDS elements content distribution and proportion data of Co@Fe MOG.

Element distribution				
Element	Line	Wt%	Wt% Sigma	At%
C	K	26.86	0.45	53.69
N	K	3.81	0.43	6.53
O	K	9.86	0.20	14.80
Fe	K	33.63	0.37	14.46
Co	K	25.84	0.37	10.53

Table S3. The Zeta potential of Co MOG, Fe MOG, and Co@Fe MOG.

Sample	Zeta (mV)
Co MOG	-1.58
Fe MOG	28.53
Co@Fe MOG	25.37

Table S4. Comparison of steady-state dynamic parameters.

Materials	Substrates	K_m (mM)	V_{max} ($10^{-8}Ms^{-1}$)	Refs
Co NPs	H_2O_2	1.14	1.72	[1]
	TMB	5.09	9.98	
Co/Fe-MOFs	H_2O_2	5.37	2.71	[2]
	TMB	3.51	7.63	
Citrate-Os NPs	H_2O_2	3.88	56.5	[3]
	TMB	0.096	41.2	
Ag@Fabric	H_2O_2	0.9	7.1	[4]
	TMB	0.27	13.6	
Fe_3O_4 NPs	H_2O_2	154	9.78	[5]
	TMB	0.098	3.44	
HRP	H_2O_2	3.7	8.71	[6]
	TMB	0.434	10.00	
Co@Fe MOG	H_2O_2	0.72	2.87	This work

	TMB	3.13	0.55

Table S5. Precision determination of H_2O_2 (n=6).

Sample	Added (μM)	Determined (μM)	RSD (%)
Day1	20	17.58	2.88
	40	39.88	3.62
	80	76.96	3.16
Day2	20	13	2.37
	40	48.42	3.76
	80	85.29	3.86
Day3	20	21.13	1.64
	40	35.92	4.42
	80	80.29	4.59

Table S6. Precision determination of CA (n=6).

Sample	Added (μM)	Determined (μM)	RSD (%)
Day1	15	7.89	3.82
	30	30.41	2.82
	50	51.42	2.61
Day2	15	12.60	1.40
	30	24.51	2.34
	50	53.34	2.41
Day3	15	13.78	1.87
	30	29.03	3.38
	50	50.42	3.47

Table S7. Determination of recovery rate of H_2O_2 in serum (n=3).

Sample	Added (μM)	Determined (μM)	RSD (%)	Recovery (%)
H_2O_2	20	19.87	2.72	99.37
	40	49.45	2.68	123.64
	80	82.37	0.56	102.96

Table S8. Determination of recovery rate of CA in green tea (n=3).

Sample	Added (μM)	Determined (μM)	RSD (%)	Recovery (%)
CA	15	12.87	0.21	85.85
	30	29.03	0.53	96.77
	50	50.82	0.43	101.65

Table S9. Comparison of different methods for detecting H_2O_2.

Materials	Method	LOD (μM)	Linear range (μM)	Refs
GO-AuNPs	Electrochemical detection	2	10-5000	[7]
GaN@ AuNPs	Electrochemical detection	2	10-100	[8]
GO-AgNPs	Electrochemical detection	7.9	100-10000	[9]
Au/PEDOT nanocomposite	Electrochemical detection	3.56	20-11600	[10]
FeNC	Colorimetric detection	4.36	10-600	[11]
GQDs/CuO	Colorimetric detection	0.17	0.5-10	[12]
N@TiO_2NPs	Colorimetric detection	2.5	10-300	[13]
Co@Fe MOG	Colorimetric detection	4.33	10-100	This work

Table S10. Comparison of different methods for detecting CA.

Materials	Method	LOD (μM)	Linear range (μM)	Refs
-	Raman Spectroscopy detection	1 mg/mL	2-20 mg/mL	[14]
$BaTiO_3$/MWCNT Composite	Electrochemical detection	61	100-10000	[15]
ZnO/CuO NCs	Electrochemical detection	21.78	150-1050	[16]
Macrocycle-based dinuclear foldamer	Fluorescence and colorimetric detection	2	0-20	[17]
Fluorescent sensor (TPE-Py)	Fluorescence detection	0.1	0-5	[18]
AgNPs	Colorimetric detection	0.21 mg/L	1-10 mg/L	[19]
Co@Fe MOG	Colorimetric detection	1.88	5-50	This work

Table S11. The MIC and MBC of *E.coil* and *S.aureus*.

	MIC	MBC
E.coil	512 μg/mL	1024 μg/mL
S.aureus	256 μg/mL	512 μg/mL

References

1. Y. Chen, H. Cao, W. Shi, H. Liu and Y. Huang, Fe–Co bimetallic alloy nanoparticles as a highly active peroxidase mimetic and its application in biosensing, *Chem Commun.* 2013, **49**, 5013-5015.
2. X. L. Zhao, J. L. Liu, F. T. Xie, T. Yang, R. Hu and Y. H. Yang, Iodide-enhanced Co/Fe-MOFs nanozyme for sensitively colorimetric detection of H_2S, Spectrochim. *Acta A Mol. Biomol. Spectrosc.* 2021, **262**, 120117.
3. S. He, L. Yang, P. Balasubramanian, S. Li, H. Peng, Y. Kuang, H. Deng and W. Chen, Osmium nanozyme as peroxidase mimic with high performance and negligible interference of O_2, *J. Mater. Chem. A.* 2020, **8**, 25226-25234.
4. M. N. Karim, S. R. Anderson, S. Singh, R. Ramanathan and V. Bansal, Nanostructured silver fabric as a free-standing nanozyme for colorimetric detection of glucose in urine, *Biosens. Bioelectron.* 2018, **110**, 8-15.
5. L. Gao, J. Zhuang, L. Nie, J. Zhang, Y. Zhang, N. Gu, T. Wang, J. Feng, D. Yang, S. Perrett and X. Yan, Intrinsic peroxidase-like activity of ferromagnetic nanoparticles, *Nat. Nanotechnol.* 2007, **2**, 577-583.
6. M. Li, D. Y. Li, Z. Y. Li, R. Hu, Y. H. Yang and T. Yang, A visual peroxidase mimicking aptasensor based on Pt nanoparticles-loaded on iron metal organic gel for fumonisin B1 analysis in corn meal, *Biosens. Bioelectron.* 2022, **209**, 114241.
7. G. H. Jin, E. Ko, M. K. Kim, V.-K. Tran, S. E. Son, Y. Geng, W. Hur and G. H. Seong, Graphene oxide-gold nanozyme for highly sensitive electrochemical

detection of hydrogen peroxide, *Sens. Actuators B Chem.* 2018, **274**, 201-209.

8. M. R. Zhang, X. Q. Chen and G. B. Pan, Electrosynthesis of gold nanoparticles/porous GaN electrode for non-enzymatic hydrogen peroxide detection, *Sens. Actuators B Chem.* 2017, **240**, 142-147.
9. E. Aparicio-Martínez, A. Ibarra, I. A. Estrada-Moreno, V. Osuna and R. B. Dominguez, Flexible electrochemical sensor based on laser scribed Graphene/Ag nanoparticles for non-enzymatic hydrogen peroxide detection, *Sens. Actuators B Chem.* 2019, **301**, 127101.
10. H. Shen, H. Liu and X. Wang, Surface construction of catalase-immobilized Au/PEDOT nanocomposite on phase-change microcapsules for enhancing electrochemical biosensing detection of hydrogen peroxide, *Appl. Surf. Sci.* 2023, **612**, 155816.
11. W. Lu, S. Chen, H. Zhang, J. Qiu and X. Liu, FeNC single atom nanozymes with dual enzyme-mimicking activities for colorimetric detection of hydrogen peroxide and glutathione, *J Materiomics.* 2022, **8**, 1251-1259.
12. L. Zhang, X. Hai, C. Xia, X.-W. Chen and J.-H. Wang, Growth of CuO nanoneedles on graphene quantum dots as peroxidase mimics for sensitive colorimetric detection of hydrogen peroxide and glucose, *Sens. Actuators B Chem.* 2017, **248**, 374-384.
13. M. Nasir, S. Rauf, N. Muhammad, M. Hasnain Nawaz, A. Anwar Chaudhry, M. Hamza Malik, S. Ahmad Shahid and A. Hayat, Biomimetic nitrogen doped titania nanoparticles as a colorimetric platform for hydrogen peroxide

detection, *J Colloid Interf Sci*. 2017, **505**, 1147-1157.

14. Z. Huang, X. Chen, Y. Li, J. Chen, J. Lin, J. Wang, J. Lei and R. Chen, Quantitative determination of citric acid in seminal plasma by using raman spectroscopy, *Appl Spectrosc*. 2013, **67**, 757-760.

15. S. Pitiphattharabun, N. Sato, G. Panomsuwan and O. Jongprateep, Electrocatalytic properties of a $BaTiO_3$/MWCNT composite for citric acid detection, *Catalysts*. 2022, **12**, 49.

16. M. M. Rahman, M. M. Alam, A. M. Asiri, S. Chowdhury and R. S. Alruwais, Sensitive detection of citric acid in real samples based on Nafion/ZnO–CuO nanocomposites modified glassy carbon electrode by electrochemical approach, *Mater Chem Phys.* 2023, **293**, 126975.

17. M. M. Rhaman, M. H. Hasan, A. Alamgir, L. Xu, D. R. Powell, B. M. Wong, R. Tandon and M. A. Hossain, Highly selective and sensitive macrocycle-based dinuclear foldamer for fluorometric and colorimetric sensing of citrate in water, *Sci. Rep.* 2018, **8**, 286.

18. C. Liu, Y. Hang, T. Jiang, J. Yang, X. Zhang and J. Hua, A light-up fluorescent probe for citrate detection based on bispyridinum amides with aggregation-induced emission feature, *Talanta*. 2018, **178**, 847-853.

19. S. Zhou, L. Kong, X. Wang, T. Liang, H. Wan and P. Wang, Colorimetric detection of citric acid as the biomarker for urolithiasis based on sodium dodecylsulfate-AgNPs with a portable CD-spectrometer, *Anal. Chim. Acta.* 2022, **1191**, 339178.